Electrochimica Acta 475 (2024) 143598

Contents lists available at ScienceDirect

Electrochimica Acta

journal homepage: www.journals.elsevier.com/electrochimica-acta

Unveiling the transport properties of protic ionic liquids: Lithium ion dynamics modulated by the anion fluorine reservoir

Giselle de Araujo Lima e Souza [a,1,*], Maria Enrica Di Pietro [a,*], Franca Castiglione [a], Patricia Fazzio Martins Martinez [b], Maleen Middendorf [c], Monika Schönhoff [c], Carla Cecilia Fraenza [d], Phillip Stallworth [d], Steven Greenbaum [d], Alessandro Triolo [e], Giovanni Battista Appetecchi [f], Andrea Mele [a,*]

[a] Department of Chemistry, Materials and Chemical Engineering "Giulio Natta", Politecnico di Milano, Piazza Leonardo da Vinci 32, Milan 20133, Italy
[b] School of Chemical Engineering, University of Campinas, Street Albert Einstein 500, Campinas 13083-852, Brazil
[c] Institute of Physical Chemistry, University of Münster, Corrensstraße 28-30, Münster 48149, Germany
[d] Department of Physics and Astronomy, Hunter College (CUNY), 695 Park Ave, New York, NY 10065. USA
[e] Istituto Struttura della Materia (ISM), Consiglio Nazionale delle Ricerche (CNR), Rome, Italy
[f] ENEA (Italian National Agency for New Technologies, Energy and Sustainable Economic Development), Department for Sustainability (SSPT), Casaccia Research Center, Via Anguillarese 301, Rome 00123, Italy

ARTICLE INFO

Keywords:
Electrolytes
Protic ionic liquids
NMR relaxation
Diffusivity
Fluorinated domains
Ionicity

ABSTRACT

Protic ionic liquids (PILs) show great potential as electrolyte components for energy storage devices. A comprehensive understanding of their transport properties must be achieved to optimize the design of safer and efficient electrolytes. This study focuses on a series of PILs based on the $DBUH^+$ cation (protonated 1,8-diazabicyclo[5,4,0]-undec-7-ene superbase) and three anions derived from strong acids: TFO^- (triflate), $IM14^-$ (perfluorobutyl-trifluoromethylsulfonylimide) and $TFSI^-$ (bis(trifluoromethylsulfonyl)imide). Neat PILs and PILs doped with LiTFO, LiIM14, and LiTFSI were studied using temperature-dependent NMR diffusion and relaxation techniques. The ionicity of these systems was also evaluated. Results revealed that the dynamic behaviour of lithium ions, as well as ionicity, strongly depend on the structural features of the anions, particularly in the case of $IM14^-$, whose main feature is the uneven distribution of the fluorinated sidegroups. The ^{19}F relaxation rates in $IM14^-$ provide insights into the rotational reorientation of that anion. DBUH-IM14 exhibited diffusion coefficients lower than the expected ones on the basis of its viscosity, likely due to fluorophilic intermolecular interactions involving the fluorinated terminal groups. The presence of Li^+ in the DBUH-IM14 electrolyte led to unexpected and relatively faster translational mobility of Li^+ ions, resulting in a higher lithium apparent transference number. However, the trends observed in ionicity indicate a more complex interplay between intermolecular interactions and ion correlations. While DBUH-TFSI showed minimal effect of Li^+ addition, DBUH-TFO and DBUH-IM14 exhibited a significant decrease in ionicity, possibly attributed to strong interactions between ions.

1. Introduction

The use of lithium ion batteries (LIBs) exponentially increased in the last decades due to their excellent performance in terms of high energy-storage capability, good cycle life, and their possibility of being manufactured in different sizes and shapes allowing the development of flexible electronic devices [1]. However, safety is still an issue because the current state-of-the-art electrolyte solutions for rechargeable LIBs are composed of a relatively thermally unstable lithium salt (usually lithium hexafluorophosphate, $LiPF_6$) dissolved in flammable carbonate organic solvents [1]. It is known that under thermal, mechanical, and/or electrical abuses of the LIB, rising temperature can initiate an exothermic process resulting in fire, explosion, and release of toxic gases [2]. Therefore, the development of safer and more efficient electrolytes

* Corresponding authors.
E-mail addresses: giselle.souza@hunter.cuny.edu (G. de Araujo Lima e Souza), mariaenrica.dipietro@polimi.it (M.E. Di Pietro), andrea.mele@polimi.it (A. Mele).
[1] Department of Physics and Astronomy, Hunter College (CUNY), 695 Park Ave, New York, NY 10065, USA

https://doi.org/10.1016/j.electacta.2023.143598
Received 24 August 2023; Received in revised form 20 October 2023; Accepted 19 November 2023
Available online 30 November 2023

for LIBs is of primary importance [3,4].

The replacement of carbonate solvents with non-flammable ionic liquids (ILs) has been intensively investigated to improve the safety of the liquid electrolytes [1]. ILs are commonly defined as molten salts displaying a melting point below 100 °C, constituted by an organic cation and an organic/inorganic anion [5,6]. Usually, ILs are recognized for their unique physical chemical properties such as good transport properties, high thermal stabilities, large electrochemical stabilities, low flammability, and low volatility [7–9]. Clearly, this set of properties makes ILs interesting candidates to replace organic solvents currently used in electrochemical devices resulting in improved safety in case of overheating/overcharging [10–12].

Depending on their chemical structure, ILs can be divided into different classes. Among them, two of the most important ones are aprotic (AILs) and protic (PILs) ionic liquids. Basically, the main difference between them is that PILs contain one (or more) exchangeable proton in the cation moiety [13], which introduces an additional level of complexity to the already rich pool of interactions of AIL-based electrolytes (Coulomb forces, hydrogen bonds, π- π interactions, dispersion forces) [8,14].

Until the last decade, most studies focused on developing ILs for LIBs electrolytes have been performed applying AILs [15]. The justification for PILs not being considered a feasible strategy for safer electrolyte components is related to the relatively low electrochemical stability and potential reactivity of the acidic proton towards alkali metals, including lithium [16]. However, in the last years, it has been demonstrated that PILs allow the realization of stable electrochemical devices with good performances comparable to those achievable with AILs [16–19]. The interest in using PILs in energy storage devices such as LIBs has then been increasing, and nowadays, PILs are quoted as promising candidates for electrolyte components by the scientific community [18,20–23].

Despite all the efforts to understand the key features ruling the properties of PILs for electrochemical applications, the dynamics of PIL-based electrolytes has been minimally discussed. So far, it is known that the presence of the acidic proton changes the intermolecular features of neat PILs, especially due to the presence of hydrogen bond networks [13, 23–25]. The scenario is even more complicated in PIL electrolytes because the addition of a third charged species, such as Li^+, may significantly affect the micro- and macroscopic properties. Still, it is unclear how the simultaneous presence of an acidic proton and a small positively charged ion changes the intermolecular network and specifically the transport properties of PIL electrolytes in terms of ion mobilities [23]. In particular, in AIL-based electrolytes, the role of the anion structure was shown to be of high relevance for Li^+ ion transport, as it determines the coordination of Li^+ to anions [26]. The role of the anion has, however, not yet been explicitly studied in AIL-based electrolytes. Therefore, this work attempts to understand the ionic and molecular mobilities of PILs formed by different anions, aiming at their application as electrolyte components. The study presents a systematic evaluation of the effects of lithium salt on the structure and dynamic properties of PILs. To this end, the present work investigated a set of PILs based on the 1,8-diazabicyclo[5,4,0]-undec-7-ene ($DBUH^+$) cation and three anions obtained from very strong acids: trifluoromethanesulfonate (TFO^-), (trifluoromethanesulfonyl-nonafluorobutylsulfonyl)imide ($IM14^-$), and bis(trifluoromethanesulfonyl)imide ($TFSI^-$) (Fig. 1). It is established that PILs are readily synthesized through a neutralization reaction between a Brønsted acid and a Brønsted base. [13] Therefore, the careful selection of precursors is vital to minimize the presence of neutral species in the bulk system. In this study, DBU was chosen as a cation precursor owing to its super-strong basicity, characterized by a large size and strong charge delocalization on the N—C═N moiety [27]. Previous studies have demonstrated that, when combined with highly potent acids like HIM14, HTFO, and HTFSI, DBU undergoes full protonation, resulting in the formation of PILs without any detectable presence of neutral species [25,28]. Both neat PILs and PIL electrolytes (PIL + lithium salt containing the same anion, i.e., LiTFO, LiIM14, and LiTFSI)

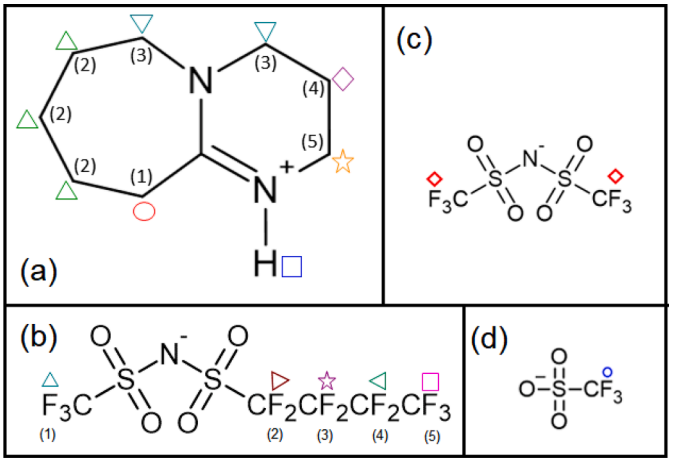

Fig. 1. Structure of the $DBUH^+$ cation and the (b) $IM14^-$, (c) $TFSI^-$ and (d) TFO^-anions. Numbers and markers correspond to the assignment of the ^1H NMR signals (for the $DBUH^+$ cation) and ^{19}F NMR signals (for the anions).

were investigated by different NMR techniques to access the rotational and translational dynamics of the ions. The combination of relaxation and diffusion NMR data provided a general picture of the ionic mobilities from the molecular bond scale to the μm scale. In addition, density and conductivity, together with the diffusion coefficients, allowed the calculation of the ionicity to characterize the ionic behavior of the systems. The synergy between these different techniques provides a complete picture of the ion dynamics in the PIL electrolytes, which turns out to be dependent on the features of the anion, especially in the case of $IM14^-$ containing systems.

2. Materials and methodology

Three PILs, DBUH-IM14, DBUH-TFSI and DBUH-TFO were prepared following a previously established protocol [25] consisting of a standard neutralization reaction (for DBUH-IM14 and DBUH-TFO) or a neutralization followed by a metathesis reaction (for DBUH-TFSI). Additional purification and vacuum-drying steps were performed. Three PIL electrolytes, $(DBUH\text{-}IM14)_1(LiIM14)_{0.1}$, $(DBUH\text{-}TFSI)_1(LiTFSI)_{0.1}$ and $(DBUH\text{-}TFO)_1(LiTFO)_{0.1}$, were prepared by doping the neat PILs with the lithium salt containing the same anion keeping the molar ratio $[DBUH^+]$:$[Li^+]$ equal to 10:1. All samples were characterized using diffusion and relaxation NMR spectroscopy. Density and electrochemical impedance spectroscopy (EIS) measurements were performed to the PIL electrolytes to allow the quantitative estimation of the ionicity. Details on sample preparation and purification, as well as characterization methods, are given in Supplementary Material.

3. Results

3.1. Translational motion of the ions

Fig. 2a displays the self-diffusion coefficient (D_i) of the ionic species in the neat PILs and PILs electrolytes (the raw data are available in the Supporting Information, Tables S1-S3, as well as the individual plots, Figures S1-S3). Experimental data were fitted by using both the Vogel-Fulcher-Tammann (VFT) type relationship [29] (Eq. S4) and the Arrhenius equation [30] (Eq. S5). The best fitting parameters are reported in Tables S4-S5, respectively.

According to the standard Stokes-Einstein equation, high diffusivity is expected for PILs with low viscosity (high fluidity), as previously reported for some DBU-based PILs [28]. The results obtained for DBUH-TFSI (85 mPa.s at 318 K) and DBUH-TFO (448 mPa.s at 318 K), the least and the most viscous system, respectively [25], are in line with

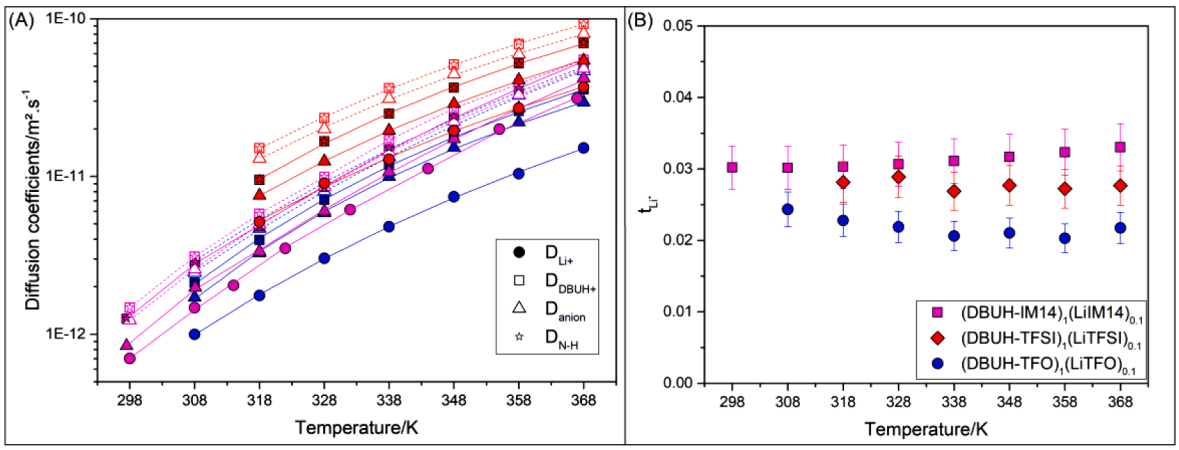

Fig. 2. (a) Self-diffusion coefficients of the DBUH-TFSI (red), DBUH-TFO (blue) and DBUH-IM14 (purple) neat PILs (hollow symbols) and PILs electrolytes (filled symbols) as a function of temperature - solid lines correspond to the VFT fitting; (b) Apparent transference number t_{Li+} for the lithium ion in the investigated PIL electrolytes.

this relationship, showing the highest and smallest translational mobility, respectively. Surprisingly, DBUH-IM14 (213 mPa.s at 318 K) behaves as an exception to the viscosity statement since its diffusivity is very close to that of DBUH-TFO (see data in Tables S1-S3), which is the most viscous system among the studied PILs. The slowing of the diffusive motion of DBUH-IM14 reasonably stems from the additional intermolecular interactions in the fluorophilic domains introduced by the $IM14^-$ anion [31,32].

In previous studies, a consistent pattern emerged, indicating a decrease in both cation and anion self-diffusion coefficients as the size of the cation increased [33]. When comparing the self-diffusion coefficients of the neat DBU-based PILs with those of guanidinium-based PILs that have similar anions, an overall reduction in mobility becomes apparent. Importantly, the measured values still fall within the same range (E-12 m^2.s), as seen in the case of CnHTMG-TFSI and CnHTMG-TFO, where $n = 1$ and 4, respectively [33].

Interesting conclusions can be drawn when evaluating the diffusion ratios (Figures S1-S3). In all the systems, the exchangeable proton (N—H) has the same diffusion coefficient as the $DBUH^+$ cation ($D_{N—H}/D_{DBUH+} \approx 1$). This indicates a charge transport based on the vehicular mechanism, in agreement with other anhydrous PILs containing similar anions (TFO^- and $TFSI^-$) [34,35]. Additionally, it also confirms the kinetic stability of the N—H bond in $DBUH^+$ [20]. Additionally, the cation/anion diffusion coefficient ratios, D_{cation}/D_{anion}, is always higher than the unity ($D_{cation}/D_{anion} > 1$), indicating that the ions of the selected PIL are not diffusing as an ion pair [36].

While D_{cation}/D_{anion} is nearly constant in the whole temperature range studied for the sulfonylimide-based PILs (DBUH-TFSI and DBUH-IM14), it decreases for DBUH-TFO (see also Fig. S3, hollow symbols), in agreement with similar findings for PIL containing the TFO^- anions [37]. With the $D_{N—H}/D_{DBUH+}$ ratio being constant in the temperature range, this indicated that TFO^- experiences a higher diffusivity enhancement with the temperature increase than the $DBUH^+$ cation. The difference between imide and triflate-based PIL can be related to the different intermolecular interactions: TFO^- has a strong and localized H-bond component which is, *per se*, very sensitive to the temperature, while $IM14^-$ and $TFSI^-$ have a more diffuse *soft* hydrogen bond network [38,39]. The different response to temperature is thus reasonable, as it is directly related to the different sensitivity of the two types of H-bond networks to temperature.

Considering the effects of the lithium salt addition, overall, the presence of Li^+ decreases the diffusion coefficients of all the PILs' ions, in agreement with results reported for other ILs doped with lithium salts [40]. Besides, the relative diffusivities follow the expected order $D_{cation} > D_{anion} > D_{Li+}$considering that the Li^+ cation is generally anion coordinated and exists as a distribution of complexes of varying sizes [41,42].

Interestingly, the diffusion ratio D_{Li+}/D_{anion} (Figures S1-S3) follows the order $D_{Li+}/D_{IM14-} > D_{Li+}/D_{TFSI-} > D_{Li+}/D_{TFO-}$. There are two main mechanisms describing Li^+ transport in ILs: the vehicular mechanism on the one hand [43], where Li^+ diffuses with its solvation shell, which was shown to consist of a number n>1 of anions [44,45], and the structural diffusion mechanism on the other hand [40], where Li^+ transport occurs through the anion exchange in the first Li^+solvation shell via the subsequent steps of disruption–diffusion–reformation of the solvation shell. MD simulations showed that the relative contributions of these two mechanisms depend on two factors: i) the Li salt concentration, with low Li^+ concentrations driving the diffusion towards the vehicular mode, high Li^+ concentrations favouring the structural diffusion pathway, and ii) the size-shape features of the anion, with large and asymmetrical anions preferring the structural diffusion mechanism [42,46,47]. In the cases reported here, with a constant salt concentration, the size and asymmetry of Li-IM14 complexes may be particularly important in selecting an efficient transport mechanism, confirming the unique effects of the distribution of the highly fluorinated $IM14^-$ anions on the overall transport of Li ions.

Additional considerations can be drawn from the translational activation energies (E_a^{transl}) extracted from the Arrhenius model (Table S5). For the DBUH-TFSI and DBUH-TFO samples, $E_a^{transl}(Li^+)$ seems to be uncorrelated to the activation energy of other species. Indeed $E_a^{transl}(Li^+) = 37.8$ kJ.mol^{-1} in the DBUH-TFSI electrolyte, slightly smaller than both cation and anion (38.4–38.5 kJ.mol^{-1}), and $E_a^{transl}(Li^+) = 42.6$ kJ.mol^{-1} for the DBUH-TFO electrolyte, smaller than both cation (44.5 kJ.mol^{-1}) and anion (45.1 kJ.mol^{-1}). Instead, for the DBUH-IM14 electrolyte $E_a^{transl}(Li^+)$ is on the upper limit (50.5 kJ.mol^{-1}), very close to the activation energy of the anion (50.2 kJ.mol^{-1}), and higher than the activation energy of the cation (48.4 kJ.mol^{-1}). Therefore, the overall picture emerging from the diffusion data suggest a relationship between the structural features of the $IM14^-$ anion and the dynamic properties observed in the corresponding electrolyte, stressing once again the unique behavior of DBUH-IM14 and its electrolyte.

The diffusion data allows one to quantify the relative mobility of Li^+ ions with respect to other species in the mixture by calculating the apparent transference number, which is the fractional contribution of an ion species to the overall conductivity [48]. Indeed, high values for Li^+ transference number are crucial for facilitating efficient charge and discharge processes in LIBs [49]. For all the studied PIL electrolytes ($x_{LiSalt} = 0.09$), it is $t_{Li+} < 0.04$ with a negligible variation when increasing the temperature, and t_{Li+} follows the order

$t_{Li+}(DBUH\text{-}IM14)_1(LiIM14)_{0.1}$ > $t_{Li+}(DBUH\text{-}TFSI)_1(LiTFSI)_{0.1}$> $t_{Li+}(DBUH\text{-}TFO)_1(LiTFO)_{0.1}$ (Fig. 2b and Table S6). This trend highlights the distinct influence of IM14 on the motion of Li ions, contrasting with TFSI and TFO. The asymmetry in IM14, coupled with its higher steric hindrance and tendency to form fluorophilic domains [32], weakens interactions with Li^+ ions. Consequently, DBUH-IM14 exhibits a higher Li transference number compared to other PILs, a feature attributed to the reduced Li-anion coordination and the lesser formation of stable clusters. This asymmetrical structure of $IM14^-$ aligns with previous observations made for other asymmetric anions such as FTFSI [44]. The low apparent transference numbers calculated for the studied PIL electrolytes are in line with transference numbers found for other mixtures of ILs and lithium salts at similar concentrations [41,50,51]. Typically, lower salt concentrations in IL-based electrolytes compared to organic solvent-based electrolytes, along with the higher viscosity and lower conductivity, contribute to the poorer rate performance of the Li-containing IL electrolytes in the same cell configuration [46]. As the salt concentration in the electrolyte increases, t_{Li+} also tends to increase to a certain extent due to the higher Li^+ availability at the electrodes, which likely is the primary reason for the improved rate capability. While bearing in mind the possible formation of multiple ions and/or ion couples occurring at high lithium contents [52], the results presented here encourage further investigations on exploring DBU-based PIL electrolytes considering higher salt concentrations.

3.2. ^1H spin–lattice relaxation times T_1: the cation rotational motion

The $DBUH^+$ cation local dynamics of the PILs and the effects of lithium doping on it was probed by spin-lattice NMR relaxation times T_1 (raw data in Tables S7-S9 in the Supplementary Material). Fig. 3a shows that for all systems R_1 (the relaxation rate, simply defined as $1/T_1$) of $DBUH^+$ protons (exemplified by the $CH_2(4)$ group) increases with increasing temperature, reaches a maximum at the temperature $T_{R1,max}$, and then decreases (individual plots in Figure S4-S6 in the Supplementary Material). This indicates that these nuclei undergo a smoothly changing from the diffusion limit (slow motion, characteristic of viscous systems and/or low temperatures and/or molecules having large size) to the extreme narrowing limit (fast motion, characteristic of fluid systems

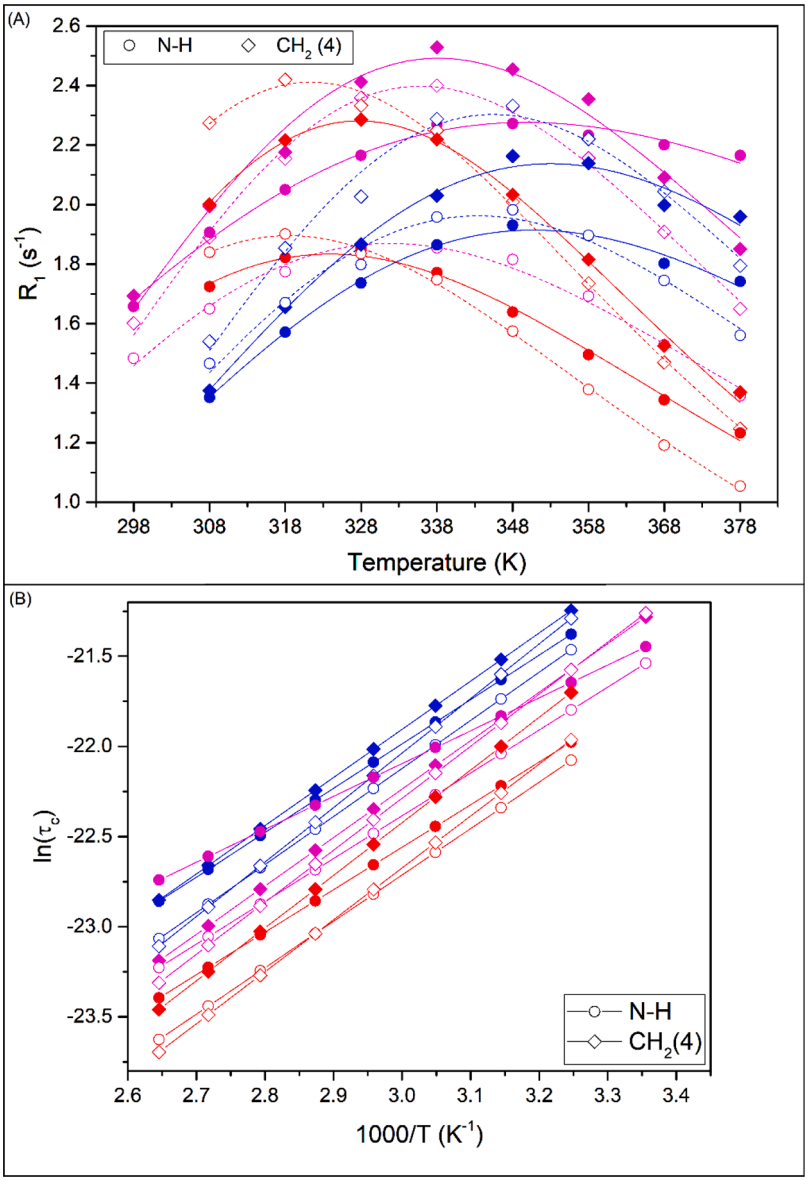

Fig. 3. (a) N—H and $CH_2(4)$ ^1H spin-lattice relaxation rates R_1 and (b) Arrhenius plot of the reorientational correlation times τ_c as a function of the temperature, obtained for the DBUH-IM14 (purple), DBUH-TFSI (red) and DBUH-TFO (blue) neat PILs (hollow symbols) and PILs electrolytes (filled symbols). Lines correspond to the data regressed using the BPP fitting parameters and (b) guide to the eyes. Assignments are shown in Fig. 1.

and/or high temperatures and/or molecules having small size) [53,54].

To obtain quantitative information about the relaxation mechanisms, the relaxation rates ^{1}H R_1 of the $DBUH^+$ were fitted through the Bloembergen, Purcell, and Pound (BPP) model [55] (Tables S10-S12). A detailed BPP model description is presented in the Section 3 of the Supplementary Material, as well as the possible physical interpretations of the calculated correlation times τ_c. As observed in Fig. 3b, as well as in Figures S7-S9, for the neat PILs, the R_1 profiles of the CH_2 groups of the $DBUH^+$ cation indicates that τ_c describes the whole molecular reorientational motion, with only minor differences coming from the contribution of local internal motions.

When considering the effects on the rotational motion of $DBUH^+$ cation upon addition of lithium salt (Fig. 3), an overall increase of the $T_{R1,max}$ values and the correlation times is observed (Tables S13-S15, Figures S4-S9). Such a phenomenon is expected due to viscosity effects, as already reported for other ILs [56]. For DBUH-TFSI and DBUH-TFO, the slowing down of the rotational motion is comparable for all the protons (i.e., all CH_2 groups and N—H of $DBUH^+$) in the temperature range evaluated, indicating that $DBUH^+$ undergoes random isotropic tumbling as a single molecular entity, and that Li^+ doping does not influence the distribution of the correlation times. Surprisingly, the DBUH-IM14 relaxation data clearly show how the presence of Li^+ has a stronger effect in decreasing the rotational mobility of the N—H proton compared to that of the methylene protons of $DBUH^+$ Figure S7). Remarkably, the curve of τ_c(N—H) and $\tau_c(CH_2)$ show a cross-over point around $T = 328$ K. The data show a selective dynamic response of the N—H site in the presence of Li^+, resulting in different activation energies, and decreasing of its internal mobility.

Comparing the effect of Li^+ in the activation energy for the rotational motion (Tables S10-S12), it seems that while E_a^{rot} of all the CH_2 protons

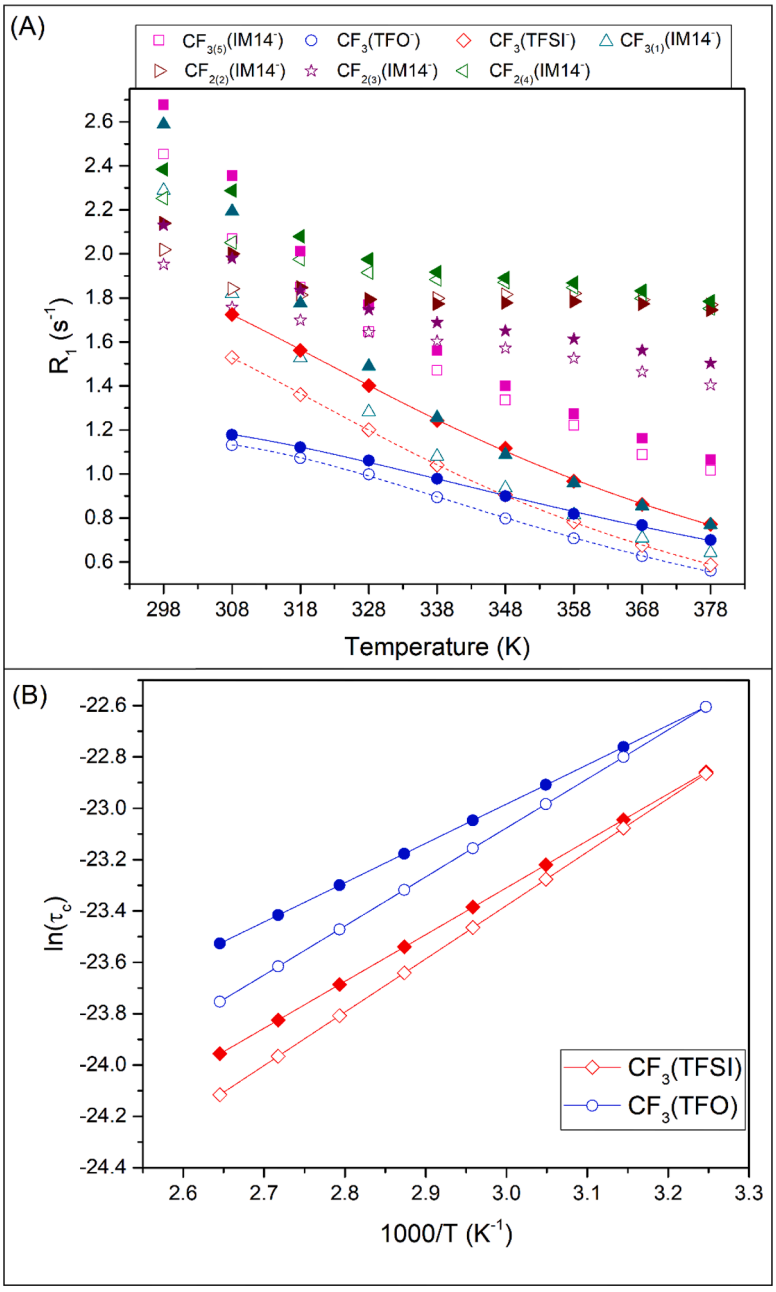

Fig. 4. (a) ^{19}F spin-lattice relaxation rates R_1 and (b) Arrhenius plot of the reorientational correlation times τ_c as a function of the temperature, measured for the DBUH-IM14, DBUH-TFSI and DBUH-TFO neat PILs (hollow symbols) and PILs electrolytes (filled symbols). Lines (a) correspond to the regressed data using the BPP fitting parameters and (b) guide to the eyes. Assignments are shown in Fig. 1.

of DBUH is nearly the same in the three neat PILs (in the range 22–25 kJ.mol^{-1}), and remains almost unchanged upon lithium addition, a significant effect on the E_a^{rot} upon lithium doping was observed only in the N—H proton of the DBUH-IM14 (ΔE_a^{rot}(N—H) = 4.6 kJ.mol^{-1}). These findings confirm the sensitivity and selectivity of the N—H locus in DBUH$^+$ towards the IM14$^-$ anion.

3.3. ^{19}F spin–lattice relaxation times T_1: the anion rotational motion

^{19}F T_1 relaxation times were measured to probe the effect of Li-doping on the anion local dynamics (Tables S16-S18). It is worth noting that the relaxation profiles do not reach the R_1 maximum, which raises concerns regarding the accuracy of the fitting parameters [46]. A detailed description of the methodology employed to ensure the effectiveness of the fitting approach is presented in the supplementary information (SI). Upon initial inspection the BPP model seems to describe quite well the relaxation profile of CF_3 groups of the DBUH-TFSI and DBUH-TFO PILs and PIL electrolytes (Fig. 4a and Table S19), considering the contribution of the internal rotation around the C3v axis as the main relaxation mechanism (see Section 3 of the Supplementary Material for more details) [57]. Fig. 4b and Tables S20-S21 show that $\tau_c(CF_3)$ DBUH-TFO > $\tau_c(CF_3)$ DBUH-TFSI, likely due to viscosity effects. In both cases, the addition of lithium salt causes an increase of R_1, more pronounced in the TFO$^-$ (Fig. 4a), and a corresponding increase of τ_c (Fig. 4b), suggesting that the ^{19}F rotational motion in the CF_3 groups was significantly reduced with respect to the neat PIL. Interestingly, this effect is stronger in the high temperature region, with τ_c at 308 K practically overlapping in the PIL and PIL electrolyte. These counterintuitive observations suggest that the good fit of the R_1 profiles to the BPP model cannot be translated automatically to a naive model of internal rotation around the C3v axis, thus calling for further refinement of the dynamic model.

The BPP model fails to describe the ^{19}F relaxation behavior of the CF_3 groups of the IM14$^-$ anion. Here, one of the trifluoromethyl groups, labeled as $CF_{3(5)}$, located at the edge of the perfluoroalkyl chain, has a shorter relaxation times than the $CF_{3(1)}$, directly attached to the sulfonylimide group (Table S16 in the Supplementary Material). Interestingly, the relaxation curves of the $CF_{3(1)}$(IM14$^-$) and CF_3(TFSI$^-$) almost overlap for T > 338 K (Fig. 4a), thus suggesting a change in the combination of relaxation mechanisms contributing to the relaxation profile, and a similarity in the relaxation mechanisms at higher temperatures between $CF_{3(1)}$(IM14$^-$) and CF_3(TFSI$^-$) in both PILs and PIL electrolytes.

Interpretation of the ^{19}F relaxation results of the CF_2 groups of IM14$^-$ (Fig. 4a) is even less straightforward because the observed R_1 dependences are changing the trend with the temperature. For clarity, R_1 vs T for $CF_{2(2)}$ shows a local minimum at ca. 322 K and a local maximum at ca. 358 K, whose interpretation is not attempted here (see Figure S10).

Concerning the effect of Li doping on ^{19}F local dynamics in both the CF_3 and CF_2 groups of the IM14$^-$ anion, Fig. 4a shows that the addition of lithium salt causes an increase of R_1, as expected.

Some general qualitative considerations on the relaxation behavior of fluorine nuclei can be drawn if one considers the R_1 profiles all together (Fig. 4a). CF_3(TFSI$^-$), CF_3(TFO$^-$) and $CF_{3(1)}$(IM14$^-$) exhibit the lowest R_1 (longest T_1) in both PILs and PIL electrolytes, and they almost overlap in the high temperature region. Given that low R_1 values qualitatively translates into short τ_C, and that for flexible molecules τ_C is a combination of molecular reorientation and internal motions (see Supplementary Material for more information), this would mean that the rotational motion of these perfluoro-methyl groups corresponds to (or is the closest to) the whole molecular reorientation. Other relaxation mechanisms add up when looking at $CF_{3(5)}$(IM14$^-$) and the CF_2 groups of IM14$^-$. Among them, spin diffusion likely plays a major role, considering the structure of the perfluorobutyl chain, and this holds true especially at low temperatures. Also, intermolecular dipole-dipole interactions may likely contribute, taking into account that IM14$^-$ is known to create fluorophilic domains in ILs [32]. Despite the assumption that different relaxation mechanisms contribute to the ^{19}F relaxation profile, any attempt to identify and quantify the relative contribution of each specific relaxation mechanism is unrealistic at present.

3.4. ^{7}Li spin–lattice relaxation times T_1: the lithium one-jump motion

The temperature dependences of R_1(Li$^+$) in the three PIL electrolytes are shown in Fig. 5a (raw data available in Table S22). A striking point is the different range of values of R_1 of Li$^+$(LiIM14) on the one hand and the other two PILs on the other hand. This indicates a large difference of the Li$^+$ local coordination environment in the case of the IM14$^-$ anion when compared to Li$^+$ in TFSI$^-$ or TFO$^-$-based electrolytes.

It should be noted that, in the case of ^{7}Li, the quadrupolar relaxation mechanism is dominating (see Section 3 of SI). In such case, the pre-factor C of the BPP model (see equations S7 and S10) depends on the electric field gradient at the site of the nucleus, and it also contains the asymmetry parameter η, dependent on the geometry of the environment at the relaxing nuclei. The C value calculated for (DBUH-IM14)$_1$(LiIM14)$_{0.1}$ is roughly 2 times higher than in the other PIL electrolytes (Table S23). A large pre-factor C might thus imply a larger electric field gradient and/or a larger asymmetry of the local Li$^+$ coordination. Bearing in mind that Li$^+$ mainly coordinates to the oxygens of the respective anions, a comparatively symmetric environment can be expected for the bidentate Li(TFSI)$_2$ coordination by four oxygens. The comparison to the ^{7}Li relaxation data in IM14$^-$ PILs, however, points out a clear role of the perfluorobutyl chain, enhancing the asymmetry of the local coordination, even though the ligand functional group able to form Li-chelates is identical in the two anions. One may conclude that with IM14 the interactions controlling the local coordination structure are less dominated by the Li-O coordination bonds, but rather the hydrophobic perfluorobutyl chain and its separation from the ionic groups imposes structural constrains and induces a more asymmetric coordination environment.

As for the Li$^+$ dynamics induced by either of the anions, again the BPP equation for quadrupolar ^{7}Li was successfully applied, and results are shown in Fig. 5b and Tables S23-S24. For quadrupolar nuclei like lithium, the correlation time and activation energy are related to the time and energy barrier for the Li$^+$ jump from one site to another [57, 58] (a more detailed description of the jump-model is in Section 3 of SI). The activation energy estimated for the Li$^+$ motion in DBUH-TFSI and DBUH-TFO was 20.4 kJ.mol^{-1} and 23.4 kJ.mol^{-1}, respectively, in line with activation energies around 20 kJ.mol^{-1} already reported for TFSI-based ILs [55,59]. Surprisingly, in the case of DBUH-IM14 electrolyte, the activation energy of Li$^+$ motion is significantly lower than in the other PILs electrolytes (E_a = 14.7 kJ.mol^{-1}). This leads to the conclusion that the large and asymmetrical IM14$^-$ anion favors the activation of local motion of the Li cation. This is consistent with the diffusion coefficient discussion of the previous section, supporting the conclusion that IM14$^-$ assists the motion of Li$^+$ ions.

Average jump distances $\langle R_{one-flip} \rangle$ were estimated from Eq. S14 and are shown in Fig. 6. The one-flip distances obtained are in the range 0.1 – 0.4 nm (Table S25) close to other Li-doped ILs reported in the literature [55,60].

$\langle R_{one-flip} \rangle$ showed an interesting increase with increasing the T value (Fig. 6). In the T < 358 K range, the order (DBUH-TFSI)$_1$(LiTFSI)$_{0.1}$ > (DBUH-TFO)$_1$(LiTFO)$_{0.1}$ > (DBUH-IM14)$_1$(LiIM14)$_{0.1}$ was observed. Notably, a cross-over occurs at T > 358 K, as the averaged one jump distance of the Li$^+$ in (DBUH-IM14)$_1$(LiIM14)$_{0.1}$ significantly exceeds that of (DBUH-TFO)$_1$(LiTFO)$_{0.1}$. This noteworthy enhancement is an actual descriptor of the different temperature response of Li$^+$ when complexed with IM14$^-$ anions, supporting the above findings that the perfluorinated chain actively modulates the dynamic behavior of Li ions, considering that Li$^+$ is always chelated by anions.

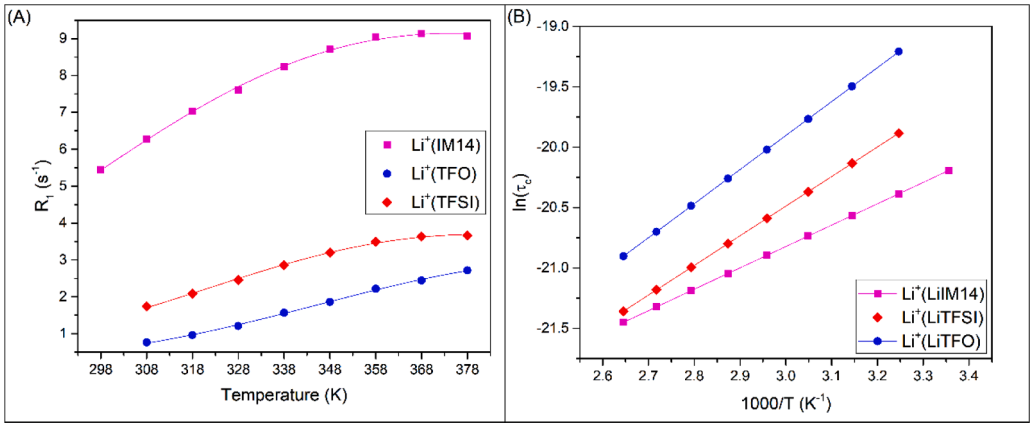

Fig. 5. (a) ^{7}Li spin-lattice relaxation rates R_1 and (b) Arrhenius plot of the reorientational correlation times τ_c as a function of the temperature measured for the DBUH-IM14, DBUH-TFSI and DBUH-TFO PILs electrolytes. Lines correspond (a) to the regressed data using the BPP fitting parameters (b) guide to the eyes.

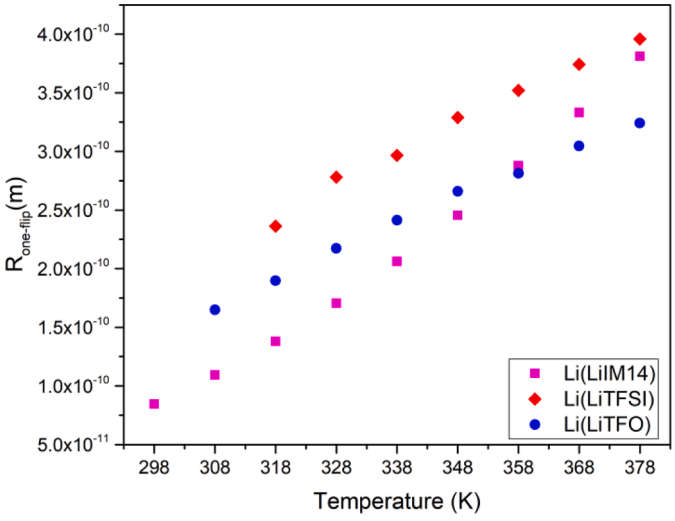

Fig. 6. Averaged Li^+ one-jump distances vs temperature dependence.

The curves of Fig. 6 show that the change of the Li one-jump distance with T is higher in the case of DBUH IM14 compared to the other two PILs. This translates into a larger response of the Li solvation shell to temperature in the PIL containing the anion with long a perfluoroalkyl chain in comparison with the other two PILs with shorter fluorinated groups. Such an enhanced sensitivity to T detected in the case of DBUH IM14 might be related to temperature-driven changes of the conformers population of the perfluorobutyl chain, in turn likely to affect the structure of the first solvation shell of the Li ions.

3.5. Density and conductivity

The temperature-dependent density (ρ) measured for the investigated PILs doped with lithium salts display the typical linear decrease with rising temperature (Tables S26-S27). The comparison of the neat PILs [25] and PIL electrolytes density (Figure S11) shows that DBUH-TFSI and DBUH-TFO are almost equally affected by the presence of the Li salt ($\Delta\rho = \rho$(PIL electrolyte) $- \rho$(PIL) $= 0.02$ g.cm^{-3}). Contrarily, the density of DBUH-IM14 is almost unchanged upon lithium doping, indicating the efficient packing ability of the $IM14^-$ anion around the cations, as previously detected for other ILs [23,42].

Considering the ionic conductivity of the neat PILs [25], we emphasize that the investigated DBU-based PILs show good ionic conductivity (i.e., in the order of 10^{-3} S.cm^{-1} at 328 K) comparable to other PILs and AILs reported in the literature [33,36,61]. Here is worth pointing out that DBUH-IM14 shows a considerable high ionic conductivity (10^{-4} S.cm^{-1}) at 298 K, which is comparable to the specific conductivity of IM14-based AILs [62].

The ionic conductivity (σ) of electrolytes is determined by the number and mobility of charge carriers throughout the system, which is, in principle, limited by the fluidity. However, our previous work has demonstrated that this does not hold for the neat PIL DBUH-IM14, for which intermolecular interactions from the anion play a key role in lowering its ionic conductivity [25]. A similar trend is observed here for the PIL electrolytes, with σ[(DBUH-TFSI)$_1$(LiTFSI)$_{0.1}$] > σ[(DBUH-TFO)$_1$(LiTFO)$_{0.1}$] > σ[(DBUH-IM14)$_1$(LiIM14)$_{0.1}$] (Table S28 and Fig. 7a). When combining the density and ionic conductivity results, some considerations can be drawn regarding the molar conductivity (Figure S12 and Table S29). The lowering in the molar conductivity due to the presence of the lithium salt is generally attributed to the Li^+ ions' interactions within the anions of the ionic liquid, which reduces the ions mobility. Indeed, Figure S12 shows that Li^+ lowers the molar conductivity of the PILs electrolytes, probably due to Li-anion coordination.

3.6. Ionicity

In an ionic system the effective fraction of ions participating in the conduction process is estimated by the ionicity [63]. In a previous work, we have demonstrated that the Walden rule fails in describing the ionicity of this set of PILs [25]. Alternatively, the ionicity can be quantitatively estimated using the inverse Haven ratio (I_{HR}), (see Supplementary Material for more information) [64–66].

The I_{HR} values calculated for the PILs and PIL electrolytes are shown in Fig. 7b and reported in Table S30. For the neat PILs, ionicity follows the order DBUH-TFSI > DBUH-IM14 ≥ DBUH-TFO. The reported values are not very high compared to AILs and PILs reported in the literature, which show considerably higher ionicity values (sometimes higher than 0.7) [33,67,68]. Noteworthy, an in-depth review revealed that for AILs, ionicity values of TFSI-containing ILs closely align with those of TFO [36]. However, this study underscores a paradigm shift for protic ionic liquids, wherein TFSI-based PILs exhibit higher ionicity compared to DBUH-TFO. In particular, the low ionicity values measured for DBUH-IM14 and DBUH-TFO may be related to interionic contributions leading to aggregations/structuration phenomena in the liquid structure [69] stemming from the different intermolecular features of the TFO^- and $IM14^-$ anions. DBUH-TFO has a well-packed cation-anion solvation shell, and a highly oriented hydrogen bonding network [39] contributing to anion-cation aggregation and decrease of ionicity. The scenario is different for the DBUH-IM14 where the weaker hydrogen bond network results in a much less structured solvation shell [39]. However, the perfluorobutyl chain is capable to generate spatial segregation, detectable as structural heterogeneities on the mesoscopic scale in

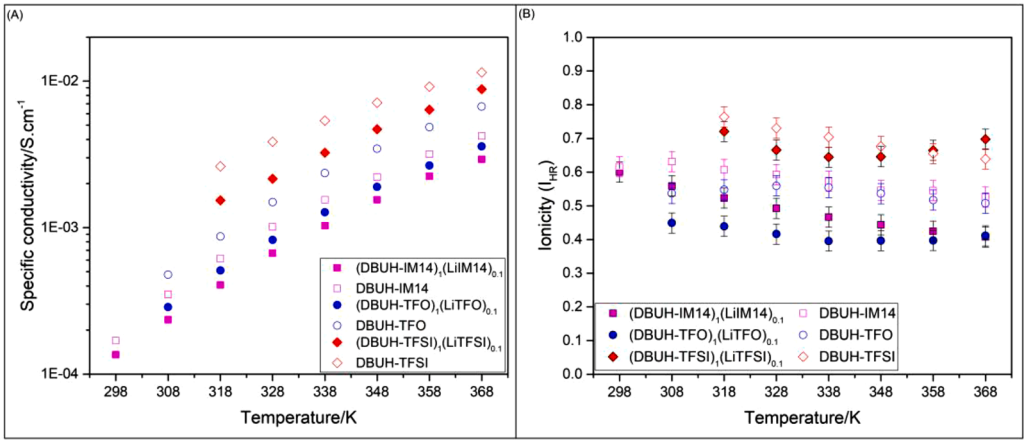

Fig. 7. (a) Ionic conductivity of the PILs and PILs electrolytes as a function of the temperature. Data for the neat PILs are available at Ref [25] (b) Ionicity (I_{HR}) vs temperature dependence calculated using the inverse Haven ratio for PILs and PIL electrolytes as a function of temperature.

perfluorinated ILs[55,56]. Such additional anion-anion intermolecular fluorophilic interaction likely contribute here to the lowering of the DBUH-IM14 ionicity, compared to DBUH-TFSI.

Considering the effect of the lithium salt on the ionicity of the PIL electrolytes (Fig. 7b filled symbols), it can be observed that (DBUH-TFSI)$_1$(LiTFSI)$_{0.1}$ is the only electrolyte in which the ionicity values of the lithium-free and doped systems are very close. Conversely, (DBUH-TFO)$_1$(LiTFO)$_{0.1}$ and (DBUH-IM14)$_1$(LiIM14)$_{0.1}$ show a relevant decrease of the ionicity with respect to the neat PILs ($\Delta I_{HR} \approx 0.1$). This difference may arise again from the nature of the intermolecular interactions. In the case of the triflate anion, Li^+ may be highly structured around TFO^- forming a strongly bonded Li—TFO, which significantly slows its rate of diffusion, contributing to the ionicity decrease.

When comparing the DBUH-TFSI and DBUH-IM14 electrolytes, the main difference between those systems lies in the size and asymmetry of the anion. Based on the findings that the $IM14^-$ anion favors Li^+ motion, it is counterintuitive to assume that [Li(IM14)$_n$] clusters are solely responsible for the decrease in ionicity. Once again, the ionicity behavior of DBUH-IM14 is linked to the known capability of $IM14^-$ to create fluorophilic domains, which introduces additional intermolecular interactions, probably enhancing anion-anion anticorrelated motion. Further progress in exploring the ionicity behavior of IM14-containing PILs can be achieved through Fast Field Cycling NMR experiments [70–74]. The application of this innovative technique is intended to gain a better understanding of the effect of correlated motions on the transport properties of IM14-based PIL and electrolytes.

4. Conclusions

Protic ionic liquid electrolytes are attractive systems to improve the safety and, in principle, the performance of lithium ions batteries. Their actual application in energy devices requires a deeper understanding of the features governing transport properties and aggregation phenomena. In particular, TFSI based anions as components of PILs are being investigated in view of possible modulation of the electrolyte response to external stimuli such as the temperature and the Li^+ doping, in the perspective of tailored electrolytes for given applications.

Beginning with DBUH-TFSI as a reference, the overall picture emerging from the present study is that of DBUH-IM14 with somewhat distinct and counterintuitive properties. Diffusion NMR highlighted lower diffusion coefficients than expected from its viscosity, probably due to occurrence of fluorophilic intermolecular interactions involving the two fluorinated terminals – CF_3 and the perfluorobutyl chain – attached to the sulfonylimide functional group of $IM14^-$. Besides, the uneven distribution of the fluorine atoms around the sulfonylimide core of IM14 anion dictates the distribution of nuclear relaxation times observed in $IM14^-$. This finding fingerprints the rotational reorientation features of $IM14^-$and suggests a descriptor for the role of the fluorinated substitute in the dynamic characterization of the electrolyte. Diffusion NMR pointed out the unexpected and relatively faster translational mobility of Li^+ in doped DBUH-IM14 electrolyte, along with the highest lithium apparent transference number. The Li^+ presence affects selectively some of the dynamic features of IM14-based PIL. Indeed, the temperature effect on the rotational correlation times τ_C of the $DBUH^+$ cation and on the $\langle R_{one-flip} \rangle$ of Li^+ marks the border between $TFSI^-$, TFO^- on the one side, and $IM14^-$ on the other. The crossover temperature detected in both cases is a physical descriptor showing the possible modulation of dynamic properties by acting on the fluorinated substituents at the $[SO_2$—-N-$SO_2]^-$ moiety.

However, the trends observed for the ionicity seem to be part of a more complex scheme. In the case of DBUH-TFSI, the ionicity seems to be barely affected by the Li^+ addition whereas for DBUH-TFO and DBUH-IM14 it shows a strong decreasing, which is probably related to the strong intermolecular created by fluorophilic domains. Overall, the findings of this work and the still open issues underlined here provide a starting point for further investigations related to this promising technology.

CRediT authorship contribution statement

Giselle de Araujo Lima e Souza: Conceptualization, Methodology, Validation, Formal analysis, Investigation, Writing – original draft, Visualization. **Maria Enrica Di Pietro:** Conceptualization, Methodology, Validation, Formal analysis, Investigation, Writing – original draft, Visualization, Supervision. **Franca Castiglione:** Writing – review & editing. **Patricia Fazzio Martins Martinez:** Investigation, Writing – review & editing. **Maleen Middendorf:** Formal analysis, Investigation, Writing – review & editing. **Monika Schönhoff:** Formal analysis, Investigation, Writing – review & editing. **Carla Cecilia Fraenza:** Formal analysis, Investigation, Writing – review & editing. **Phillip Stallworth:** Investigation, Writing – review & editing. **Steven Greenbaum:** Supervision, Writing – review & editing. **Alessandro Triolo:** Writing – review & editing. **Giovanni Battista Appetecchi:** Formal analysis, Investigation, Supervision, Writing – review & editing. **Andrea Mele:** Resources, Supervision, Writing – original draft.

Declaration of Competing Interest

The authors declare that they have no known competing financial interests or personal relationships that could have appeared to influence the work reported in this paper.

Acknowledgments

The authors thank the Regione Lombardia and ENEA for the grant for G.A.L.S. Ph.D. programme (Accordo attuativo Regione Lombardia - Enea modificato con DGR 5321/2021); M.M. thanks the Federal State of Northrhine Westphalia for funding through the International Graduate School BACCARA (Battery Chemistry, Characterization, Analysis, Recycling and Application); the portion of the work conducted at Hunter College was supported as part of the Breakthrough Electrolytes for Energy Storage (BEES), an Energy Frontier Research Center funded by the U.S. Department of Energy, Office of Science, Basic Energy Sciences under Award #: DE-SC0019409; the portion of the work conducted at ISM-CNR was supported by the project ECS00000024 "Ecosistemi dell'Innovazione"— Rome Technopole of the Italian Ministry of University and Research, public call n. 3277, PNRR— Mission 4, Component 2, Investment 1.5, financed by the European Union, Next GenerationEU.

Supplementary materials

Supplementary material associated with this article can be found, in the online version, at doi:10.1016/j.electacta.2023.143598.

References

[1] M. Armand, P. Axmann, D. Bresser, M. Copley, K. Edström, C. Ekberg, D. Guyomard, B. Lestriez, P. Novák, M. Petranikova, W. Porcher, S. Trabesinger, M. Wohlfahrt-Mehrens, H. Zhang, Lithium-ion batteries – Current state of the art and anticipated developments, J. Power Sources. 479 (2020) 26, https://doi.org/10.1016/j.jpowsour.2020.228708.

[2] P. Jaumaux, J. Wu, D. Shanmukaraj, Y. Wang, D. Zhou, B. Sun, F. Kang, B. Li, M. Armand, G. Wang, Non-Flammable liquid and quasi-solid electrolytes toward highly-safe alkali metal-based batteries, Adv. Funct. Mater. 31 (2020), 2008644, https://doi.org/10.1002/adfm.202008644.

[3] J.T. Frith, M.J. Lacey, U. Ulissi, A non-academic perspective on the future of lithium-based batteries, Nat. Commun. 14 (2023), https://doi.org/10.1038/s41467-023-35933-2.

[4] F.M.N.U. Khan, M.G. Rasul, A.S.M. Sayem, N.K. Mandal, Design and optimization of lithium-ion battery as an efficient energy storage device for electric vehicles: a comprehensive review, J. Energy Storage 71 (2023), 108033, https://doi.org/10.1016/j.est.2023.108033.

[5] C. Chiappe, D. Pieraccini, Ionic liquids: solvent properties and organic reactivity, J. Phys. Org. Chem. 18 (2005) 275–297, https://doi.org/10.1002/poc.863.

[6] N.V. Plechkova, K.R. Seddon, Applications of ionic liquids in the chemical industry, Chem. Soc. Rev. 37 (2008) 123–150, https://doi.org/10.1039/b006677j.

[7] J.S. Wilkes, A short history of ionic liquids - From molten salts to neoteric solvents, Green Chem 4 (2002) 73–80, https://doi.org/10.1039/b110838g.

[8] T. Welton, Ionic liquids: a brief history, Biophys. Rev. 10 (2018) 691–706, https://doi.org/10.1007/s12551-018-0419-2.

[9] D.R. MacFarlane, N. Tachikawa, M. Forsyth, J.M. Pringle, P.C. Howlett, G. D. Elliott, J.H. Davis, M. Watanabe, P. Simon, C.A. Angell, Energy applications of ionic liquids, Energy Environ. Sci. 7 (2014) 232–250, https://doi.org/10.1039/c3ee42099j.

[10] G.B. Appetecchi, M. Montanino, S. Passerini, Ionic liquid-based electrolytes for high energy, safer lithium batteries, in: Proc. ACS Symp. Ser., 2012, pp. 67–128, https://doi.org/10.1021/bk-2012-1117.ch004.

[11] X. Tang, S. Lv, K. Jiang, G. Zhou, X. Liu, Recent development of ionic liquid-based electrolytes in lithium-ion batteries, J. Power Sources. 542 (2022), 231792, https://doi.org/10.1016/j.jpowsour.2022.231792.

[12] G. Choudhary, J. Dhariwal, M. Saha, S. Trivedi, M.K. Banjare, R. Kanaoujiya, K. Behera, Ionic liquids: environmentally sustainable materials for energy conversion and storage applications, Environ. Sci. Pollut. Res. (2023), https://doi.org/10.1007/s11356-023-25468-w.

[13] T.L. Greaves, C.J. Drummond, Protic ionic liquids: evolving structure-property relationships and expanding applications, Chem. Rev. 115 (2015) 11379–11448, https://doi.org/10.1021/acs.chemrev.5b00158.

[14] K. Fumino, R. Ludwig, Analyzing the interaction energies between cation and anion in ionic liquids: the subtle balance between Coulomb forces and hydrogen bonding, J. Mol. Liq. 192 (2014) 94–102, https://doi.org/10.1016/j.molliq.2013.07.009.

[15] K. Karuppasamy, J. Theerthagiri, D. Vikraman, C.J. Yim, S. Hussain, R. Sharma, T. Maiyalagan, J. Qin, H.S. Kim, Ionic liquid-based electrolytes for energy storage devices: a brief review on their limits and applications, Polymers (Basel) 12 (2020) 1–37, https://doi.org/10.3390/POLYM12040918.

[16] T. Stettner, A. Balducci, Protic ionic liquids in energy storage devices: past, present and future perspective, Energy Storage Mater. 40 (2021) 402–414, https://doi.org/10.1016/j.ensm.2021.04.036.

[17] N. Böckenfeld, M. Willeke, J. Pires, M. Anouti, A. Balducci, On the use of lithium iron phosphate in combination with protic ionic liquid-based electrolytes, J. Electrochem. Soc. 160 (2013) A559–A563, https://doi.org/10.1149/2.027304jes.

[18] T. Vogl, S. Menne, R.S. Kühnel, A. Balducci, The beneficial effect of protic ionic liquids on the lithium environment in electrolytes for battery applications, J. Mater. Chem. A. 2 (2014) 8258–8265, https://doi.org/10.1039/c3ta15224c.

[19] S. Menne, J. Pires, M. Anouti, A. Balducci, Protic ionic liquids as electrolytes for lithium-ion batteries, Electrochem. Commun. 31 (2013) 39–41, https://doi.org/10.1016/j.elecom.2013.02.026.

[20] T. Stettner, F.C. Walter, A. Balducci, Imidazolium-Based Protic Ionic Liquids as Electrolytes for Lithium-Ion Batteries, (2019) 55–59. https://doi.org/10.1002/batt.201800096.

[21] T. Stettner, S. Gehrke, P. Ray, B. Kirchner, A. Balducci, Water in protic ionic liquids: properties and use of a new class of electrolytes for energy-storage devices, ChemSusChem. 12 (2019) 3827–3836, https://doi.org/10.1002/cssc.201901283.

[22] T. Vogl, C. Vaalma, D. Buchholz, M. Secchiaroli, R. Marassi, S. Passerini, A. Balducci, The use of protic ionic liquids with cathodes for sodium-ion batteries, J. Mater. Chem. A. 4 (2016) 10472–10478, https://doi.org/10.1039/c6ta02277d.

[23] A.T. Nasrabadi, V. Ganesan, Structure and transport properties of lithium-doped aprotic and protic ionic liquid electrolytes: insights from molecular dynamics simulations, J. Phys. Chem. B. 123 (2019) 5588–5600, https://doi.org/10.1021/acs.jpcb.9b04477.

[24] M.S. Miran, H. Kinoshita, T. Yasuda, M.A.B.H. Susan, M. Watanabe, Hydrogen bonds in protic ionic liquids and their correlation with physicochemical properties, Chem. Commun. 47 (2011) 12676–12678, https://doi.org/10.1039/c1cc14817f.

[25] G. De Araujo Lima E Souza, M.E. Di Pietro, F. Castiglione, P.H. Marques Mezencio, P.Fazzio Martins Martinez, A. Mariani, H.M. Schütz, S. Passerini, M. Middendorf, M. Schönhoff, A. Triolo, G.B. Appetecchi, A. Mele, Implications of anion structure on physicochemical properties of DBU-based protic ionic liquids, J. Phys. Chem. B. 126 (2022) 7006–7014, https://doi.org/10.1021/acs.jpcb.2c02789.

[26] M. Brinkkötter, E.I. Lozinskaya, D.O. Ponkratov, P.S. Vlasov, M.P. Rosenwinkel, I. A. Malyshkina, Y. Vygodskii, A.S. Shaplov, M. Schönhoff, Influence of anion structure on ion dynamics in polymer gel electrolytes composed of poly(ionic liquid), ionic liquid and Li salt, Electrochim. Acta. 237 (2017) 237–247, https://doi.org/10.1016/j.electacta.2017.03.219.

[27] J. Nowicki, M. Muszyński, J.P. Mikkola, Ionic liquids derived from organosuperbases: en route to superionic liquids, RSC Adv. 6 (2016) 9194–9208, https://doi.org/10.1039/c5ra23616a.

[28] M.S. Miran, H. Kinoshita, T. Yasuda, M.A.B.H. Susan, M. Watanabe, Physicochemical properties determined by ΔpK a for protic ionic liquids based on an organic super-strong base with various Brønsted acids, Phys. Chem. Chem. Phys. 14 (2012) 5178–5186, https://doi.org/10.1039/c2cp00007e.

[29] K.R. Harris, M. Kanakubo, Revised and extended values for self-diffusion coefficients of 1-alkyl-3-methylimidazolium tetrafluoroborates and hexafluorophosphates: relations between the transport properties, J. Phys. Chem. B. 120 (2016) 12937–12949, https://doi.org/10.1021/acs.jpcb.6b10341.

[30] K.J. Laidler, The development of the arrhenius equation, J. Chem. Educ. 61 (1984) 494–498, https://doi.org/10.1021/ed061p494.

[31] A. Triolo, F. Lo Celso, C. Ottaviani, P. Ji, G.B. Appetecchi, F. Leonelli, D.S. Keeble, O. Russina, Structural features of selected protic ionic liquids based on a super-strong base, Phys. Chem. Chem. Phys. 21 (2019) 25369–25378, https://doi.org/10.1039/c9cp03927a.

[32] O. Russina, F. Lo Celso, M. Di Michiel, S. Passerini, G.B. Appetecchi, F. Castiglione, A. Mele, R. Caminiti, A. Triolo, Mesoscopic structural organization in triphilic room temperature ionic liquids, Faraday Discuss 167 (2013) 499–513, https://doi.org/10.1039/c3fd00056g.

[33] D. Rauber, F. Philippi, J. Zapp, G. Kickelbick, H. Natter, R. Hempelmann, Transport properties of protic and aprotic guanidinium ionic liquids, RSC Adv 8 (2018) 41639–41650, https://doi.org/10.1039/C8RA07412G.

[34] J.W. Blanchard, J.P. Belières, T.M. Alam, J.L. Yarger, G.P. Holland, NMR determination of the diffusion mechanisms in triethylamine-based protic ionic liquids, J. Phys. Chem. Lett. 2 (2011) 1077–1081, https://doi.org/10.1021/jz200357j.

[35] N. Yaghini, L. Nordstierna, A. Martinelli, Effect of water on the transport properties of protic and aprotic imidazolium ionic liquids-an analysis of self-diffusivity, conductivity, and proton exchange mechanism, Phys. Chem. Chem. Phys. 16 (2014) 9266–9275, https://doi.org/10.1039/c4cp00527a.

[36] O. Nordness, J.F. Brennecke, Ion dissociation in ionic liquids and ionic liquid solutions, Chem. Rev. 120 (2020) 12873–12902, https://doi.org/10.1021/acs.chemrev.0c00373.

[37] V. Overbeck, H. Schröder, A.M. Bonsa, K. Neymeyr, R. Ludwig, Insights into the translational and rotational dynamics of cations and anions in protic ionic liquids by means of NMR fast-field-cycling relaxometry, Phys. Chem. Chem. Phys. 23 (2021) 2663–2675, https://doi.org/10.1039/d0cp05440b.

[38] A. Triolo, A. Paolone, A. Sarra, F. Trequattrini, O. Palumbo, G. Battista Appetecchi, F. Lo Celso, P. Chater, O. Russina, Structure and vibrational features of the protic ionic liquid 1,8-diazabicyclo[5.4.0]-undec-7-ene-8-ium bis (trifluoromethanesulfonyl)amide, [DBUH][TFSI], J. Mol. Liq. 347 (2021), 117981, https://doi.org/10.1016/j.molliq.2021.117981.

[39] A. Triolo, F. Lo Celso, C. Ottaviani, P. Ji, G.B. Appetecchi, F. Leonelli, D.S. Keeble, O. Russina, Structural features of selected protic ionic liquids based on a super-strong base, Phys. Chem. Chem. Phys. 21 (2019) 25369–25378, https://doi.org/10.1039/c9cp03927a.

[40] F. Chen, M. Forsyth, Elucidation of transport mechanism and enhanced alkali ion transference numbers in mixed alkali metal-organic ionic molten salts, Phys. Chem. Chem. Phys. 18 (2016) 19336–19344, https://doi.org/10.1039/c6cp01411a.

[41] G.A. Giffin, A. Moretti, S. Jeong, K. Pilar, M. Brinkkötter, S.G. Greenbaum, M. Schönhoff, S. Passerini, Connection between lithium coordination and lithium diffusion in [Pyr12O1][FTFSI] ionic liquid electrolytes, ChemSusChem. 11 (2018) 1981–1989, https://doi.org/10.1002/cssc.201702288.
[42] J.B. Haskins, W.R. Bennett, J.J. Wu, D.M. Hernández, O. Borodin, J.D. Monk, C. W. Bauschlicher, J.W. Lawson, Computational and experimental investigation of li-doped ionic liquid electrolytes: [pyr14][TFSI], [pyr13][FSI], and [EMIM][BF4], J. Phys. Chem. B. 118 (2014) 11295–11309, https://doi.org/10.1021/jp5061705.
[43] O. Borodin, G.D. Smith, W. Henderson, Li+ cation environment, transport, and mechanical properties of the LiTFSI doped N-methyl-N-alkylpyrrolidinium+TFSI- Ionic liquids, J. Phys. Chem. B. 110 (2006) 16879–16886, https://doi.org/10.1021/jp061930t.
[44] M. Brinkkötter, G.A. Giffin, A. Moretti, S. Jeong, S. Passerini, M. Schönhoff, Relevance of ion clusters for Li transport at elevated salt concentrations in [Pyr12O1][FTFSI] ionic liquid-based electrolytes, Chem. Commun. 54 (2018) 4278–4281, https://doi.org/10.1039/c8cc01416g.
[45] M. Gouverneur, F. Schmidt, M. Schönhoff, Negative effective Li transference numbers in Li salt/ionic liquid mixtures: does Li drift in the "wrong" direction? Phys. Chem. Chem. Phys. 20 (2018) 7470–7478, https://doi.org/10.1039/c7cp08580j.
[46] P. Nürnberg, E.I. Lozinskaya, A.S. Shaplov, M. Schönhoff, Li coordination of a novel asymmetric anion in ionic liquid-in-Li salt electrolytes, J. Phys. Chem. B. 124 (2020) 861–870, https://doi.org/10.1021/acs.jpcb.9b11051.
[47] A. Wettstein, D. Diddens, A. Heuer, Controlling Li+ transport in ionic liquid electrolytes through salt content and anion asymmetry: a mechanistic understanding gained from molecular dynamics simulations†, Phys. Chem. Chem. Phys. 24 (2022) 6072–6086, https://doi.org/10.1039/d1cp04830a.
[48] M. Gouverneur, J. Kopp, L. Van Wüllen, M. Schönhoff, Direct determination of ionic transference numbers in ionic liquids by electrophoretic NMR, Phys. Chem. Chem. Phys. 17 (2015) 30680–30686, https://doi.org/10.1039/c5cp05753a.
[49] H. Ye, J. Huang, J.J. Xu, A. Khalfan, S.G. Greenbaum, Li ion conducting polymer gel electrolytes based on ionic liquid/PVDF-HFP blends, J. Electrochem. Soc. 154 (2007) A1048, https://doi.org/10.1149/1.2779962.
[50] F. Castiglione, E. Ragg, A. Mele, G.B. Appetecchi, M. Montanino, S. Passerini, Molecular environment and enhanced diffusivity of Li+ ions in lithium-salt-doped ionic liquid electrolytes, J. Phys. Chem. Lett. 2 (2011) 153–157, https://doi.org/10.1021/jz101516c.
[51] K. Hayamizu, Y. Aihara, H. Nakagawa, T. Nukuda, W.S. Price, Ionic conduction and ion diffusion in binary room-temperature ionic liquids composed of [emim][BF4] and LiBF4, J. Phys. Chem. B. 108 (2004) 19527–19532, https://doi.org/10.1021/jp0476601.
[52] S. Zugmann, M. Fleischmann, M. Amereller, R.M. Gschwind, H.D. Wiemhöfer, H. J. Gores, Measurement of transference numbers for lithium ion electrolytes via four different methods, a comparative study, Electrochim. Acta. 56 (2011) 3926–3933, https://doi.org/10.1016/j.electacta.2011.02.025.
[53] M.E. Di Pietro, F. Castiglione, A. Mele, Polar/apolar domains' dynamics in alkylimidazolium ionic liquids unveiled by the dual receiver NMR 1H and 19F relaxation experiment, J. Mol. Liq. 322 (2021), 114567, https://doi.org/10.1016/j.molliq.2020.114567.
[54] M.E. Di Pietro, K. Goloviznina, A. Van Den Bruinhorst, G. De Araujo Lima E Souza, M. Costa Gomes, A.A.H. Padua, A. Mele, Lithium salt effects on the liquid structure of choline chloride-urea deep eutectic solvent, ACS Sustain. Chem. Eng. 10 (2022) 11835–11845, https://doi.org/10.1021/acssuschemeng.2c02460.
[55] K. Hayamizu, S. Tsuzuki, S. Seki, Y. Umebayashi, Nuclear magnetic resonance studies on the rotational and translational motions of ionic liquids composed of 1-ethyl-3-methylimidazolium cation and bis(trifluoromethanesulfonyl)amide and bis (fluorosulfonyl)amide anions and their binary systems including li, J. Chem. Phys. 135 (2011), https://doi.org/10.1063/1.3625923.
[56] K. Hayamizu, S. Tsuzuki, S. Seki, Transport and electrochemical properties of three quaternary ammonium ionic liquids and lithium salts doping effects studied by NMR spectroscopy, J. Chem. Eng. Data. 59 (2014) 1944–1954, https://doi.org/10.1021/je500065k.
[57] K. Hayamizu, S. Tsuzuki, S. Seki, Molecular motions and ion diffusions of the room-temperature ionic liquid 1,2-dimethyl-3-propylimidazolium bis (trifluoromethylsulfonyl)amide (DMPImTFSA) studied by1H, 13C, and19F NMR, J. Phys. Chem. A. 112 (2008) 12027–12036, https://doi.org/10.1021/jp802392t.
[58] A. Carof, M. Salanne, T. Charpentier, B. Rotenberg, On the microscopic fluctuations driving the NMR relaxation of quadrupolar ions in water, J. Chem. Phys. 143 (2015), https://doi.org/10.1063/1.4935496.
[59] S. Tsuzuki, K. Hayamizu, S. Seki, Y. Ohno, Y. Kobayashi, H. Miyashiro, Quaternary ammonium room-temperature ionic liquid including an oxygen atom in side chain/lithium salt binary electrolytes: ab initio molecular orbital calculations of interactions between ions, J. Phys. Chem. B. 112 (2008) 9914–9920, https://doi.org/10.1021/jp803866u.
[60] K. Hayamizu, S. Tsuzuki, S. Seki, K. Fujii, M. Suenaga, Y. Umebayashi, Studies on the translational and rotational motions of ionic liquids composed of N -methyl- N -propyl-pyrrolidinium (P13) cation and bis(trifluoromethanesulfonyl)amide and bis(fluorosulfonyl)amide anions and their binary systems including lithium salts, J. Chem. Phys. 133 (2010), https://doi.org/10.1063/1.3505307.
[61] M. Hasani, S.A. Amin, J.L. Yarger, S.K. Davidowski, C.A. Angell, Proton transfer and ionicity: an 15N NMR study of pyridine base protonation, J. Phys. Chem. B. 123 (2019) 1815–1821, https://doi.org/10.1021/acs.jpcb.8b10632.
[62] G.B. Appetecchi, M. Montanino, M. Carewska, M. Moreno, F. Alessandrini, S. Passerini, Chemical-physical properties of bis(perfluoroalkylsulfonyl)imide-based ionic liquids, Electrochim. Acta. 56 (2011) 1300–1307, https://doi.org/10.1016/j.electacta.2010.10.023.
[63] D.R. MacFarlane, M. Forsyth, E.I. Izgorodina, A.P. Abbott, G. Annat, K. Fraser, On the concept of ionicity in ionic liquids, Phys. Chem. Chem. Phys. 11 (2009) 4962–4967, https://doi.org/10.1039/b900201d.
[64] H. Tokuda, S. Tsuzuki, M.A.B.H. Susan, K. Hayamizu, M. Watanabe, How ionic are room-temperature ionic liquids? An indicator of the physicochemical properties, J. Phys. Chem. B. 110 (2006) 19593–19600, https://doi.org/10.1021/jp064159v.
[65] K. Ueno, H. Tokuda, M. Watanabe, Ionicity in ionic liquids: correlation with ionic structure and physicochemical properties, Phys. Chem. Chem. Phys. 12 (2010) 1649–1658, https://doi.org/10.1039/c001176m.
[66] K. Ueno, K. Yoshida, M. Tsuchiya, N. Tachikawa, K. Dokko, M. Watanabe, Glyme-lithium salt equimolar molten mixtures: concentrated solutions or solvate ionic liquids? J. Phys. Chem. B. 116 (2012) 11323–11331, https://doi.org/10.1021/jp307378j.
[67] H. Srour, M. Traïkia, B. Fenet, H. Rouault, M.F. Costa Gomes, C.C. Santini, P. Husson, Effect of nitrile-functionalization of imidazolium-based ionic liquids on their transport properties, both pure and mixed with lithium salts, J. Solution Chem. 44 (2015) 495–510, https://doi.org/10.1007/s10953-014-0280-2.
[68] F. Philippi, D. Rauber, J. Zapp, R. Hempelmann, Transport properties and ionicity of phosphonium ionic liquids, Phys. Chem. Chem. Phys. 19 (2017) 23015–23023, https://doi.org/10.1039/c7cp04552b.
[69] R. Ludwig, The effect of dispersion forces on the interaction energies and far infrared spectra of protic ionic liquids, Phys. Chem. Chem. Phys. 17 (2015) 13790–13793, https://doi.org/10.1039/c5cp00885a.
[70] D. Kruk, M. Wojciechowski, Y.L. Verma, S.K. Chaurasia, R.K. Singh, Dynamical properties of EMIM-SCN confined in a SiO2 matrix by means of 1H NMR relaxometry, Phys. Chem. Chem. Phys. 19 (2017) 32605–32616, https://doi.org/10.1039/c7cp06174a.
[71] D. Kruk, R. Meier, E.A. Rössler, Nuclear magnetic resonance relaxometry as a method of measuring translational diffusion coefficients in liquids, Phys. Rev. E - Stat. Nonlinear, Soft Matter Phys. 85 (2012) 1–5, https://doi.org/10.1103/PhysRevE.85.020201.
[72] D. Kruk, E. Masiewicz, S. Lotarska, R. Markiewicz, S. Jurga, Correlated dynamics in ionic liquids by means of NMR relaxometry: butyltriethylammonium bis (trifluoromethanesulfonyl)imide as an example, Int. J. Mol. Sci. 22 (2021) 1–13, https://doi.org/10.3390/ijms22179117.
[73] D. Kruk, E. Masiewicz, S. Lotarska, R. Markiewicz, S. Jurga, Relationship between translational and rotational dynamics of alkyltriethylammonium-based ionic liquids, Int. J. Mol. Sci. 23 (2022), https://doi.org/10.3390/ijms23031688.
[74] C.C. Fraenza, S.G. Greenbaum, Broadband NMR relaxometry as a powerful technique to study molecular dynamics of ionic liquids, ChemPhysChem (2023), 202300268, https://doi.org/10.1002/cphc.202300268.